Combined Targeting of the BRD4–NUT–p300 Axis in NUT Midline Carcinoma by Dual Selective Bromodomain Inhibitor, NEO2734

Chevaun D. Morrison-Smith[1], Tatiana M. Knox[1], Ivona Filic[1], Kara M. Soroko[2], Benjamin K. Eschle[2], Margaret K. Wilkens[2], Prafulla C. Gokhale[2], Francis Giles[3], Andrew Griffin[4], Bill Brown[5], Geoffrey I. Shapiro[6], Beth E. Zucconi[7], Philip A. Cole[7], Madeleine E. Lemieux[8], and Christopher A. French[1]

ABSTRACT

NUT midline carcinoma (NMC) is a rare, aggressive subtype of squamous carcinoma that is driven by the BRD4-NUT fusion oncoprotein. BRD4, a BET protein, binds to chromatin through its two bromodomains, and NUT recruits the p300 histone acetyltransferse (HAT) to activate transcription of oncogenic target genes. BET-selective bromodomain inhibitors have demonstrated on-target activity in patients with NMC, but with limited efficacy. P300, like BRD4, contains a bromodomain. We show that combining selective p300/CBP and BET bromodomain inhibitors, GNE-781 and OTX015, respectively, induces cooperative depletion of MYC and synergistic inhibition of NMC growth. Treatment of NMC cells with the novel dual p300/CBP and BET bromodomain–selective inhibitor, NEO2734, potently inhibits growth and induces differentiation of NMC cells *in vitro*; findings that correspond with potentiated transcriptional effects from combined BET and p300 bromodomain inhibition. In three disseminated NMC xenograft models, NEO2734 provided greater growth inhibition, with tumor regression and significant survival benefit seen in two of three models, compared with a lead clinical BET inhibitor or "standard" chemotherapy. Our findings provide a strong rationale for clinical study of NEO2734 in patients with NMC. Moreover, the synergistic inhibition of NMC growth by CBP/p300 and BET bromodomain inhibition lays the groundwork for greater mechanistic understanding of the interplay between p300 and BRD4-NUT that drives this cancer.

Introduction

NUT midline carcinoma (aka NUT carcinoma, NMC) is a rare subtype of squamous carcinoma, first described by our group (1, 2), that is defined by rearrangement of the *NUT* gene (also known as *NUTM1*). NMC is perhaps the most aggressive solid tumor in humans with a median survival of 6.5 months (3), and there exist no effective or standard treatment regimens. With a median age of 23.6 (4), NMC is a disease of adolescent and young adults (AYA), a vulnerable cancer population with poorer outcomes than their adult counterparts (5). Thus, NMC, an orphan disease with no treatment, represents an unmet need that urgently requires effective therapy.

Of all the genomic rearrangements observed for *NUTM1*, it is most commonly fused to *BRD4* (3, 6, 7; 78%). Existing data suggest that the resulting protein, BRD4-NUT, is the single driver of NMC, with few if any additional oncogenic mutations (8). BRD4-NUT is therefore an attractive therapeutic target.

BRD4-NUT drives tumor growth by blocking differentiation through the upregulation of MYC (9), a powerful oncoprotein in high-grade cancers. BRD4-NUT binds chromatin through the dual bromodomains of BRD4 (9), a member of the BET family of chromatin readers that recognize and bind acetylated histones. The NUT moiety of BRD4-NUT recruits the histone acetyltransferase (HAT), p300, to chromatin and forms massive megabase-sized (≤2 MB) histone regions called megadomains (10). Megadomains are enriched in histone marks associated with active transcription, including H3K9Ac, H3K14Ac, H3K36Me, and the mark associated with active enhancers that is selectively acetylated by p300 and CBP, H3K27Ac (11). Megadomains drive the expression of associated genes, including *MYC*, a key megadomain oncogenic target in all NMCs analyzed (9, 10, 12, 13). Thus, BRD4-NUT–driven NMC should properly be thought of as an epigenetic disease. BET inhibitors that are highly selective for the dual acetyl-histone–binding bromodomains of BET proteins have been tested for NMC therapy. Although the first-in-human compounds have demonstrated on-target activity in patients with NMC, a narrow therapeutic window has limited their efficacy (14, 15).

To improve upon the efficacy of BET bromodomain inhibitors (BETi) in targeting BRD4-NUT, we sought to explore rational combination strategies. A recent CRISPR screen determined that upregulation of cell-cycle genes can overcome BETi-induced growth arrest of NMC cells and pharmacologic CDK4/6 inhibition could overcome this resistance (16). Indeed, it was found that palbociclib, a CDK4/6 inhibitor, was synergistic with BETi *in vitro* and *in vivo*; however, the survival benefit after 21-day treatment of this combination was not durable (median survival = 34 days). Here, we investigated the

[1]Department of Pathology, Brigham and Women's Hospital, Harvard Medical School, Boston, Massachusetts. [2]Experimental Therapeutics Core and Belfer Center for Applied Cancer Science, Dana-Farber Cancer Institute, Boston, Massachusetts. [3]Developmental Therapeutics Consortium, Chicago, Ilinois. [4]Praxis Precision Medicines, Cambridge, Massachusetts. [5]Paraza Pharma Inc., Montreal, Quebec, Canada. [6]Department of Medical Oncology, Dana Farber Cancer Institute, Harvard Medical School, Boston, Massachusetts. [7]Department of Medicine, Division of Genetics, Brigham and Women's Hospital and Department of Biological Chemistry and Molecular Pharmacology, Harvard Medical School, Boston, Massachusetts. [8]Bioinfo, Plantagenet, Ontario, Canada.

Note: Supplementary data for this article are available at Molecular Cancer Therapeutics Online (http://mct.aacrjournals.org/).

Corresponding Author: Christopher A. French, M.D., Brigham and Women's Hospital/Harvard Medical School, New Research Building Rm. 630G, 77 Avenue Louis Pasteur, Boston, MA 02115. Phone: 617-525-4415; Fax: 617-525-4422; E-mail: cfrench@bwh.harvard.edu

Mol Cancer Ther 2020;19:1406–14

doi: 10.1158/1535-7163.MCT-20-0087

therapeutic potential of cotargeting p300, a known interactor with BRD4-NUT that is thought to be critical to its oncogenic function.

Results

Combined BET and p300/CBP bromodomain inhibition synergistically inhibits NMC growth

Previously, we have shown that one of a limited number of unique interactors with BRD4-NUT that do not also interact with the BRD4 portion is p300 (13). NUT341-598 associates with the TAZ2 domain of p300 and activates its HAT activity *in vitro* (12), a feature that may explain the transcriptional activating properties of NUT (17), and hyperacetylation of megadomains (10). We reasoned that a strategy cotargeting two distinct members of the BRD4-NUT core complex, such as p300 and BRD4, may exhibit synergistic inhibition of BRD4-NUT function. Available to us was the latest generation p300/CBP bromodomain inhibitor, GNE-781, which exhibits a >5,600-fold greater affinity for the CBP/p300 bromodomain (IC_{50} = 0.9 nmol/L) over that of BRD4 (IC_{50} = 5.1 μmol/L; ref. 18). The p300 bromodomain has been described as important for its chromatin occupancy (19), protein–protein interactions (20), and even HAT activity (21). We found that GNE-781 treatment exhibited selective growth inhibition of BRD4-NUT+ NMC cell lines, TC-797 (22), 10–15 (9), and PER-403 (23) with low nanomolar potency, although limited efficacy, compared with non-NMC cell lines, COS7, U2OS, and 293T (**Fig. 1A** and **B**). Growth of the non-NMC cell lines was so unaffected by GNE-781 that we could not calculate IC_{50} values (**Fig. 1A**). In contrast, these lines were all sensitive to the clinical BET inhibitor, OTX015 (birabresib), as expected (**Fig. 1C** and **D**; refs. 14, 15). We demonstrated that combining sub-IC_{50} concentrations of either OTX015 or GNE-781 were both synergistic in inhibiting growth of the two NMC cell lines tested, PER-403 and TC-797 (**Fig. 1E**), using combination indices calculated by Chou-Talalay (24) methods. The finding indicated that inhibiting p300/CBP and BET bromodomains is synergistic in repressing growth of NMC cells.

The p300/CBP and BET bromodomain inhibitors, NEO2734 and NEO1132, induce differentiation and G_1-phase cell-cycle arrest

A novel class of compounds, developed by Epigene Therapeutics, Montreal, Canada, bind the bromodomains of both epigenetic readers (such as BET proteins) and writers (such as chromatin post-translational modifiers; ref. 25). Two compounds with these properties include the tool molecule, NEO1132, and the structurally unrelated clinical lead, NEO2734 (also known as EP31670, **Fig. 2A**). The synthetic steps for these compounds abstracted from patents US20180237417A1 (NEO2734; ref. 26), and WO2017024408A1 (NEO1132; ref. 27) are included in Supplementary Methods. NEO2734 has recently been reported to potently inhibit prostate cancer growth *in vitro* and *in vivo*, including in SPOP-mutated tumors, which exhibit high-level resistance to BET inhibitors (25).

In cell-free assays, NEO2734 was determined by Epigene to bind both BET bromodomains with 2–10 fold higher affinity than the clinical selective BET inhibitor i-BET-762 (molibresib; ref. 28), GSK-762), and to p300/CBP bromodomains at low nanomolar IC_{50}

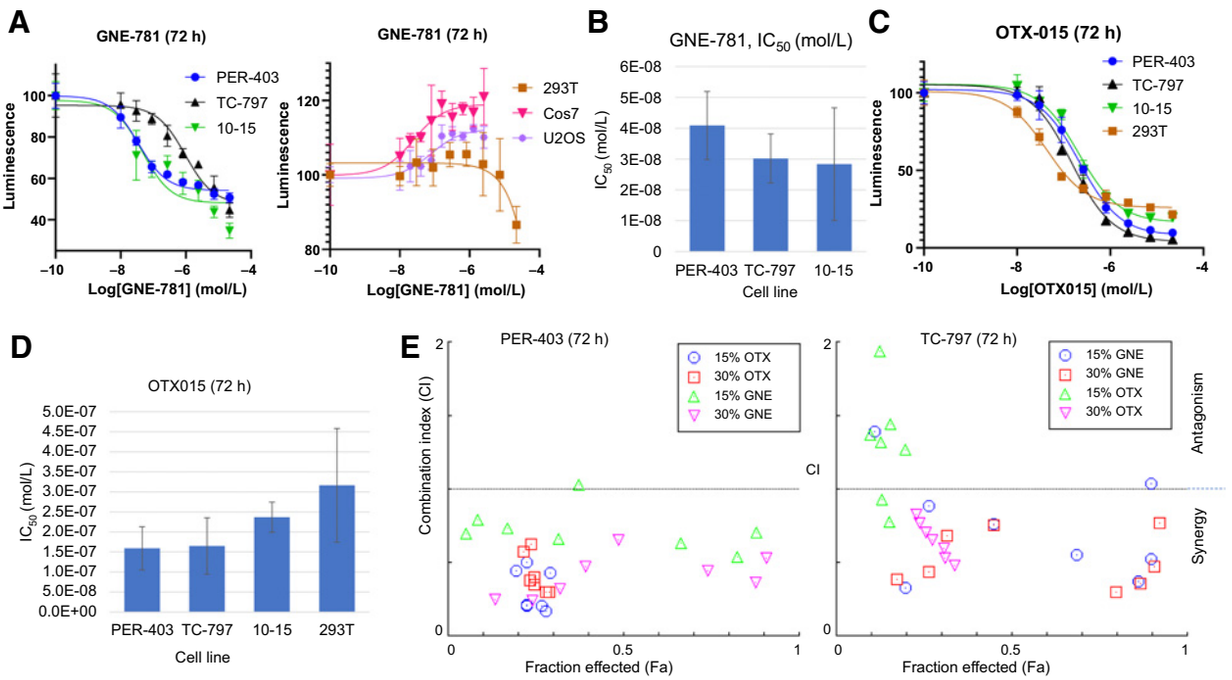

Figure 1.

BET and p300/CBP bromodomain inhibition synergistically repress growth of NUT midline carcinoma cells. **A,** Dose–response curves of cell viability based on ATP content as measured by CellTiter-Glo luminescence. All experiments were performed in biologic triplicates, each in technical triplicate. Shown are representative curves, each from a single biologic replicate. **B,** Bar graph of IC_{50} values calculated on the basis of the average of biologic triplicates from the experiment depicted in **A**. **C,** Dose–response curves performed as described in **A**. **D,** Average IC_{50} values calculated from three biologic replicates from **C**. **E,** Combination index plots generated by CompuSyn software (http://www.combosyn.com/feature.html) used to calculate synergistic versus antagonistic activity combining GNE-781 with OTX015. This experiment was performed in biologic duplicate using technical triplicates; results shown represent a single biologic replicate. Abbreviations: GNE, GNE-781; OTX, OTX015.

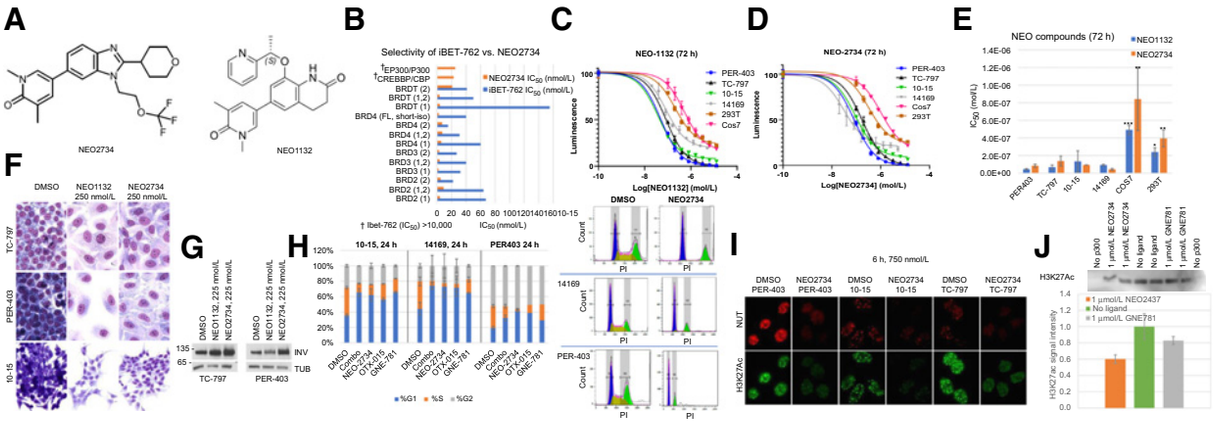

Figure 2.

NEO1132 and NEO2734 potently induce differentiation and growth arrest following depletion of acetylated BRD4-NUT foci in NUT midline carcinoma cells. **A,** Structures of NEO2734 and NEO1132. **B,** Comparison of the binding affinity of NEO2734 with that of iBET-762 to p300/CBP and a variety of BET bromodomains determined by BROMOscan. **C** and **D,** Dose–response curves performed as described in **Fig. 1A** using technical triplicates for each of three biologic replicates. **E,** Bar graph of IC_{50} values averaged from **C** and **D**. *, $P < 0.005$; **, $P < 1 \times 10^{-5}$; ***, $P < 0.5 \times 10^{-6}$ comparing the indicated cell line with all NMC cell line IC_{50} values combined. **F,** Hemacolor-stained NMC cell lines grown on coverslips incubated with the indicated compounds for 72 hours. All images were taken at 400× with the same exposure. **G,** Immunoblot of two NMC cell lines following 72-hour incubation with the indicated compounds. **H,** Flow cytometric cell-cycle analysis of NMC cells incubated with the listed compounds for 24 hours. Combo, combined GNE-781 (62.5 nmol/L) and OTX015 (62.5 nmol/L). Left, cell-cycle fractions; right, representative histograms. Each experiment was performed in two biologic replicates. PI, propidium iodide. **I,** Coimmunofluorescence microscopy of three NMC cell lines exposed to NEO2734 (750 nmol/L) or DMSO for 6 hours, and stained with anti-NUT and anti-H3K27Ac antibodies. All images were taken at 1,000× magnification with identical exposure settings per condition. **J,** Histone acetyltransferase assay using purified p300 and nucleosomes. Top, immunoblot of a representative experiment showing H3K27ac. Bottom, quantitative analysis showing averages and standard deviation from three biologic replicates, each performed with technical duplicates.

values (**Fig. 2B**). Treatment of the four NMC cell lines with either NEO1132 or NEO2734 inhibited growth with similar potency and efficacy as with OTX015 (**Fig. 2C–E**). NMC cell lines as a group were significantly more sensitive than the non-NMC cell lines, COS7 and 293T, to these compounds (**Fig. 2C–E**). The similar effects of two structurally unrelated NEO compounds supports the idea that these phenotypes result from on-target effects of both molecules.

NEO1132 and NEO2734 rapidly induced squamous differentiation in NMC cell lines, as evidenced by morphologic flattening, enlargement, and nuclear pallor (**Fig. 2F**), and expression of the terminal squamous differentiation marker, involucrin (**Fig. 2G**), or keratins (Supplementary Fig. S1), an effect previously observed with BRD4-NUT knockdown (29), BET (30, 31) or BRD4-selective bromodomain inhibition (9). The differentiation phenotype corresponds with induction of G_1–cell-cycle arrest of NMC cells, a response that is also seen with BET, p300/CBP, and combined bromodomain inhibition (**Fig. 2H**). Apoptosis appears to be minor if not nonexistent in response to any of the compound treatments based on lack of PARP cleavage or an identifiable apoptotic population seen by flow cytometry (**Fig. 2H**; Supplementary Fig. S2). The findings support the idea that cellular differentiation, not death, is the dominant response to bromodomain inhibition in NMC.

Chromatin immunoprecipitation (ChIP) by Yan (25) and colleagues previously demonstrated that NEO2734 has BET and p300/CBP-bromodomain–like effects on chromatin in SPOP-mutated prostate cancer models, decreasing BRD4 and acetyl-H3 enrichment at select enhancers and promoters. In keeping with this activity, we observed rapid diminishment of BRD4-NUT and associated H3K27Ac immunofluorescent foci (which correspond with megadomains), in three NMC cell lines treated with NEO2734 (**Fig. 2I**). The decrease in BRD4-NUT immunofluorescence is likely due to spreading and/or eviction from chromatin from BET inhibition, rather than decrease in overall protein levels, because Western blot analysis revealed only a mild decrease in overall BRD4-NUT protein levels (Supplementary Fig. S3).

Previous studies have suggested that engagement of the bromodomain of p300 with ligand (acetylated histones or small-molecule inhibitors) can increase (21) or decrease (32) its HAT activity. Thus, as with the p300/CBP bromodomain inhibitor, CBP112 (21), it is possible that ligand binding of the p300 bromodomain by GNE-781 or NEO2734 might modify acetylation of the p300-specific substrate, H3K27. Indeed, while global H3K27 acetylation in NMC cells appeared unaffected by NEO2734 (Supplementary Fig. S4), both GNE-781 and NEO2734 ligands modestly inhibit acetylation of H3K27 on purified nucleosomes in the presence of recombinant full-length p300 (**Fig. 2J**). The H3K27Ac depletion by NEO2734 is evidence of p300/CBP-selective inhibition by this compound as with GNE-781, and because global changes in H3K27Ac are not seen, we speculate that H3K27Ac depletion is occuring selectively within megadomains, where p300 is enriched. Hyperacetylation, including that of H3K27, within BRD4-NUT megadomains is a hallmark of NMC (ref. 10; **Fig. 2I**), and is likely required for the upregulation of BRD4-NUT transcriptional targets, such as MYC. Thus, inhibition of acetylation selectively within megadomains by NEO2734 may potentiate the BET bromodomain inhibitory effects of this compound.

The transcriptional changes induced by NEO2734 on NMC cells resemble those of an enhanced BET bromodomain inhibition–like effect

We sought to determine the early effects on genome-wide transcription upon treatment of NMC cells with NEO2734, and to determine what contribution p300/CBP and BET bromodomain inhibition makes to these changes. To do so, we needed to establish the earliest time point where effects on distribution of

BRD4-NUT/H3K27Ac are seen, and the minimum doses of each compound required to achieve the maximal effect on transcription of select genes. We established that the earliest time point when the disappearance of BRD4-NUT/H3K27Ac foci was maximal upon NEO2734 exposure was 6 hours, based on a time course (Supplementary Fig. S5). We next determined the minimal dose of GNE-781, OTX015, combined GNE-781 and OTX015, and NEO2734 required to induce the maximal effect on transcription of select genes after 6 hours as detected by quantitative RT-PCR. Four genes were chosen whose expression increases ($n = 2$) or decreases ($n = 2$) significantly upon exposure of NMC cells to BET bromodomain inhibition (10). The dose determined to achieve near-maximal change in transcription by OTX015 was 500 nmol/L, for GNE-781 and NEO2734 it was 1 μmol/L, and notably, for combined OTX015 and GNE-781, it was only 62.5 nmol/L for each (**Fig. 3A** and **B**). The up to 16-fold increased potency on transcription upon combining OTX015 and GNE-781 over either alone, at equivalent doses, indicates a synergistic effect of p300/CBP and BET bromodomain inhibition on transcription of select genes.

Using the above conditions for transcriptional analysis, we performed RNA sequencing on PER-403 and TC-797 NMC cells. Heatmaps depicting all differentially expressed genes relative to DMSO control (**Fig. 3C**) are remarkable, first, for a greater fold change seen globally in genes from both cell lines treated with NEO2734 compared with other compounds and combinations. Second, comparison of differentially expressed (DE) genes (**Fig. 3D**), and quality control analyses (Supplementary Fig. S6) reveal that there is a large degree of overlap in differentially expressed genes (compared with DMSO control) between all compound treatments (GNE-781, NEO2734, OTX-015, and OTX015+GNE-781), in both cell lines, and between cell lines (**Fig. 3C**, bottom). Third, these analyses (**Fig. 3C** and **D**; Supplementary Fig. S6) also reveal that changes induced by NEO2734, although showing some distinct p300/CBP bromodomain inhibition–like effects (**Fig. 3D**, pink, yellow, and green highlighted overlaps), most closely resemble those by combined OTX015 and GNE-781, or OTX015 treatment alone, indicating a predominantly BET bromodomain inhibition–like effect. The finding suggests that, rather than inducing divergent transcriptional effects, the p300/CBP bromodomain inhibition activity of NEO2734 may synergize with BET inhibition to affect convergent biological pathways.

Consistent with the concept that BET and p300/CBP bromodomain inhibition affects similar pathways, GSEA using Hallmark and Gene Ontology (GO) gene sets reveals abundant overlap between transcriptional programs that are changed across different compounds (**Fig. 3E**). It is notable, however, that only OTX015, NEO2734, or OTX015 + GNE-781 induce squamous differentiation, indicating that p300/CBP bromodomain inhibition has no effect on this pathway. We speculate that the lack of squamous differentiation induced by GNE-781 may explain its comparative lack of efficacy in inducing full growth arrest (**Fig. 1A**). Also remarkable is that all treatments resulted in MYC target pathway downregulation (**Fig. 3E**), a key target of BRD4-NUT. Downregulation of MYC targets is attributable at least in part to decreased MYC protein abundance. Treatment with NEO2734 results in greater loss of MYC protein than either OTX015, GNE-781, or a combination thereof (**Fig. 3F**). Importantly, a synergistic or at least additive effect was observed by combining p300/CBP and BET bromodomain inhibition in decreasing MYC levels to below that which is observed with either treatment alone (**Fig. 3G**), supporting the idea that the NEO2734-induced MYC depletion may result from the potentiated effect of dual p300/CBP and BET bromodomain inhibition.

While the data indicate a mostly BET bromodomain inhibitor–like effect of NEO2734, there are other factors that may contribute to the efficacy of NEO2734, because there are numerous differentially expressed genes seen only with NEO2734 treatment (**Fig. 3D**). We investigated the possibility that the changes in expression of genes induced by NEO2734 also changed upon exposure to other compounds, but were lower than our cutoff (3-fold change, FDR ≤ 0.05). Indeed, volcano plots reveal that the majority of differentially expressed "NEO2734-only" genes were also up- or downregulated in the OTX015, or GNE-781+OTX015 treatment groups, and a minority in the GNE-781 group, but did not meet our cutoffs (**Fig. 3H**). This finding helps explain the discrepancy between overlap of differentially expressed genes and transcriptional pathways affected in NEO2734 and GNE-781+OTX015–treated samples (**Fig. 3D** and **E**). Taken together, the findings reveal similar transcriptional changes induced by all compounds and combinations, but that NEO2734 induced more potent changes in differentially expressed genes.

The findings above indicate that the effects of p300/CBP bromodomain inhibition by NEO2734 potentiate those of BET bromodomain inhibition. We next asked whether the effects of NEO2734 preferencially affect BRD4-NUT–associated transcriptional programs, as does BET bromodomain inhibition (10). To resolve this question, we sought to determine whether or not downregulated genes were enriched within megadomains (e.g., **Fig. 3I**). Using previously mapped megadomains in TC-797 and PER-403 cells (10), we quantified the proportion of significant transcriptional changes in megadomain-associated genes versus those of genes that do not overlap megadomains (**Fig. 3I**). We found that all compounds and combinations, including NEO2734, induced enrichment of megadomain-associated genes among the genes downregulated by the treatments (**Fig. 3I**; Supplementary Fig. S7). The observation is meaningful because it supports the idea that p300/CBP and BET bromodomain inhibition affect overlapping epigenetically defined regions of chromatin; thus dual inhibition of these proteins might cooperatively inhibit BRD4-NUT–associated transcription.

NEO2734 inhibits growth and prolongs survival in preclinical xenograft models significantly more than BET bromodomain inhibition or "standard" chemotherapy

Given the evidence for synergistic effects of NEO2734 on transcription and growth of NMC cells, we sought to compare its efficacy *in vivo* with that of the lead clinical BET bromodomain inhibitor, i-BET-762 (molibresib; ref. 28; GSK-762), and chemotherapy that is often administered to patients with NMC, cisplatin/etoposide. We developed three xenograft models of NMC in NOD scid gamma (NSG) or NOD rag gamma (NRG) immunosuppressed mice where tumor cells are injected by tail vein, and tumor disseminates to solid organs (ovary, liver, bone marrow, brain) and bone marrow within 1–2 weeks. Our disseminated models of NMC more closely mimick the human disease, which is highly metastatic to solid organs and often presents with stage IV disease (3, 4), than previous flank-injection models (**Fig. 4A**; refs. 31, 33). The three BRD4-NUT^{+} NMC cell lines used, 14169, PER-403, and 10–15, have been stably transduced with a FUW-Luc-mCh-puro plasmid that constitutively expresses luciferase and is used to measure tumor burden by bioluminescence imaging (BLI).

We initially piloted ($n = 4$ mice per arm) NEO2734 and NEO1132 compared with clinically relevant doses of i-BET-762 established by GSK investigators for treatment of solid tumors (34), i-BET-762 combined with EP, and EP alone, in the PER-403 model. Treatment was initiated one week after cell implantation and continued for

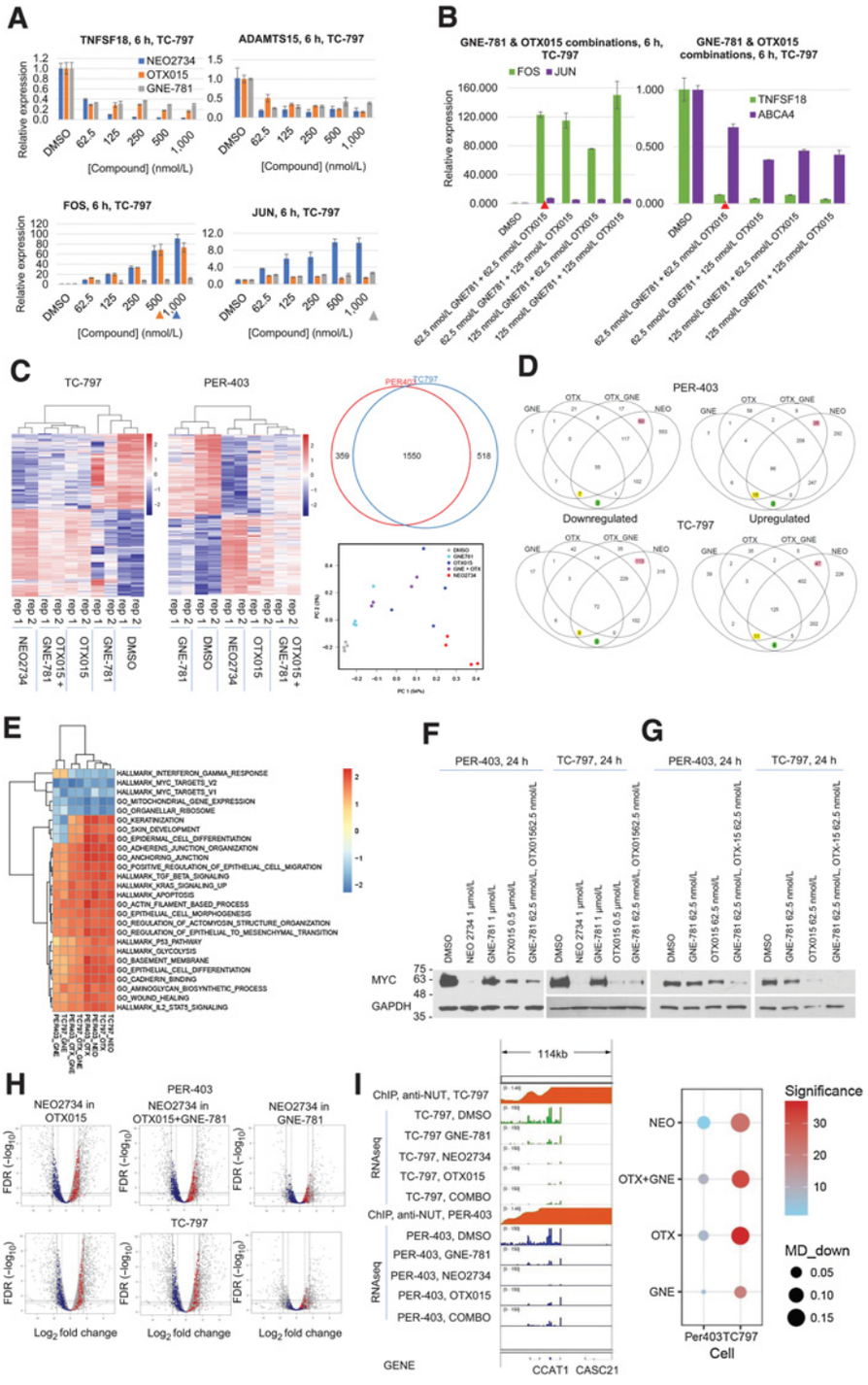

Figure 3.

The transcriptional changes induced by NEO2734 resemble overlapping effects of BET and p300/CBP inhibition, with an overall augmented BET bromodomain-like effect. **A,** qRT-PCR of the indicated genes used to determine doses of each compound to be used for RNA sequencing. Experiments were performed in biologic duplicates using technical triplicates for each. Shown are results of a single representative experiment. Arrowheads, color coded to match the corresponding compound, indicate the minimum doses of each compound at which the maximal transcriptional effect was achieved. These doses were used for RNAseq. **B,** qRT-PCR performed as in **A** to determine the doses used for combining OTX015 and GNE-781. Red arrowhead indicates the minimum dose at which near-maximal transcriptional change was attained. This dose was used for RNA sequencing. **C,** Left, heatmap of RNA sequencing results depicting all differentially expressed (DE) genes compared with DMSO for each of the indicated NMC cell lines and treatment groups. Treatment was done for 6 hours and performed in biologic duplicate. Top, right, Venn diagram of any DE gene from any treatment compared with DMSO in both cell lines. (*Continued on the following page.*)

28 days after which treatment was stopped. Mouse tumor burden and survival continued to be monitored to evaluate the durability of response after the cessation of treatment. Both NEO compounds exhibited greater growth suppression, and NEO2734 provided markedly improved survival compared with EP, i-BET-762, and even iBET-762+EP by day 100 following initiation of treatment (**Fig. 4B** and **C**). In contrast with all other treatments, NEO2734 caused tumor regression (**Fig. 4B**). Indeed, two of the three mice treated with NEO2734 were alive by day 100 (**Fig. 4C**).

With the encouraging results, we proceeded to perform a full study ($n = 8$ mice per arm) in our three mouse models comparing NEO2734, used at the clinically relevant dose found to be safe in monkeys (equivalent to 8 mg/kg/day in mice), with i-BET-762 and EP. First, all treatments, including NEO2734, were well tolerated for the duration of treatment (**Fig. 4D**). Two of the three models, PER-403 and 14169, exhibited similar responses to NEO2734 to that seen in the pilot, with regression of tumor growth seen up to day 37/30 in both models, respectively, compared with exponential tumor growth observed in mice administered i-BET-762 (GSK-762), EP, or DMSO (**Fig. 4E** and **I**). Survival was significantly greater in NEO2734 (8 mg/kg) treated PER-403 and 10–15 mice (**Fig. 4F** and **H**); median survivals were >100 days (d) ($P < 0.0001$, Supplementary Table S1) and 44 days ($P = 0.0034$, Supplementary Table S2), compared with 41.5 days and 36.5 days for i-BET-762 in these mice, respectively. In the PER-403 model, 37.5% (3/8) of mice were alive at day 115, compared with 100% mortality by day 50 in the non-NEO2734 treatment groups (**Fig. 4F**). Even a lower dose (5 mg/kg) of NEO2734 provided greater growth repression and significant survival benefit ($P = 0.0002$, **Fig. 4E** and **F**; Supplementary Table S1) than any of the non-NEO2734 treatments in the PER-403 model. The addition of EP to NEO2734, although well tolerated (Supplementary Fig. S8), did not provide significant survival benefit over NEO2734 alone in the 10–15 model (**Fig. 4H**). As in the 10–15 and PER-403 models, treatment of 14169s with NEO2734 demonstrated significantly improved survival compared with vehicle control ($P = 0.0004$, Supplementary Table S3), and at day 59, is conferring greater survival benefit than any other treatment, with 100% survival compared with 62.5%, 37.5%, and 12.5% survival in GSK-762, EP, and vehicle-treated groups, respectively (**Fig. 4J**).

To determine the pharmakodynamic activity of NEO2734 compared with vehicle and GSK-762, we performed histology and IHC on samples from each group from PER-403 and 10–15 mouse models after three days of treatment (**Fig. 4K**; Supplementary Fig. S9). There was a significant decrease in Ki-67 proliferation indices in tumor tissues of both mouse models treated with either NEO2734 or GSK-762. Likewise, there was a signficant depletion of MYC in tumors of in both mouse models treated with NEO2734, whereas there was almost no depletion in the 10–15 model tumors treated with GSK-762. Moreover, the decrease in both Ki-67 and MYC was significantly greater in tissue from both mouse models treated with NEO2734 than from GSK-762–treated mice (**Fig. 4K**). Cleaved PARP (cPARP, Supplementary Fig. S9) was not increased in any of the treatment samples compared with vehicle, correlating with our *in vitro* observations (Supplementary Fig. S2). NUT appeared somewhat depleted in the NEO2734-treated PER-403 and 10–15 mice, but definitive evaluation was precluded by background staining of hepatocytes (Supplementary Fig. S9). In summary, NEO2734 induced significantly greater loss of MYC and arrested growth than either vehicle or GSK-762 in both mouse models of NMC.

Discussion

NMC is one of the most aggressive solid tumors known, with an overall mortality exceeding 90% (4), and is second only to anaplastic thyroid carcinoma in its aggressiveness (35). Although rare, a next-generation sequencing study of 14,107 consecutive solid malignancies found that NMC comprised 0.06% of these tumors (36), bringing estimates of its annual incidence in the United States to ∼1,150 (7). Thus, NMC is not only lethal without a treatment, but vastly underdiagnosed. More effective targeted therapy for this disease is expected to improve outcomes, incentivize diagnostic testing, expand awareness, and ultimately result in earlier intervention.

Our findings indicate that NEO2734 is more effective *in vivo* than previously described targeted therapeutics in NMC, and is a promising new potential therapy for this disease. Of particular importance is our observation that tumor regression occurred in two of three of our mouse models treated with NEO2734, whereas this was not seen with any of the other treatments, including i-BET-762, or in previous studies of targeted inhibitors used at clinically relevant doses (33, 37). Even the addition of chemotherapy to i-BET-762 achieved markedly lower efficacy than NEO2734 treatment alone (**Fig. 4B**). These findings, coupled with the survival benefit of NEO2734, are promising indicators that it would outperform BET bromodomain inhibitors in patients, potentially exceeding the 20%–30% partial response rate seen with these molecules (15, 28).

There are several possible explanations for the superior *in vivo* activity of NEO2734 compared with selective BET bromodomain inhibitors, including the following: (i) synergistic inhibition of BRD4-NUT function by cotargeting p300 and BET bromodomains, both core members of the BRD4-NUT oncogenic complex; (ii)

(*Continued.*) Bottom, right, principal component analysis (PCA) of DE genes common between TC-797 and PER-403 cells for each treatment replicate compared with DMSO. **D,** Venn diagrams depicting overlap of DE genes identified by RNA sequencing between the different treatment groups for the two NMC cell lines. DE genes common to NEO2734 and the OTX015+GNE-781 combination are highlighted pink; those common to NEO2734 and GNE-781 alone and GNE-781+OTX015 combined are highlighted yellow; those common to NEO2734 and GNE-781 only are highlighted green. **E,** Heatmap of row-scaled NES for Hallmark or Genome Ontology (GO) gene sets with family-wise error < 0.25 in comparisons by GSEA of preranked $\log_2$ fold change in any treatment group relative to DMSO control. **F** and **G,** Immunoblots following 24-hour exposure to the indicated compounds and concentrations. **H,** Volcano plots depicting expression changes in other treatment groups of genes deemed to be DE only in NEO2734-treated samples (3-fold change, solid vertical line, and FDR = 0.05, solid horizontal line). Gray dots are the values for the underlying dataset (e.g., in "NEO2734 in OTX015", the gray dots are the values for the OTX015 dataset. Red dots are upregulated DE genes identified in the NEO2734-only treated cells; blue dots are those that are downregulated). Dashed vertical lines indicate 2-fold change in expression. Dashed horizontal line indicates FDR = 0.1. **I,** Left, IGV snapshot of *CCAT1* within the *MYC* regulatory region (Chr. 8) showing ChIPseq (orange, from Alekseyenko and colleagues, 2015, GSE70870) and corresponding RNA sequencing (green and blue) peaks for TC-797 and PER-403 cell lines treated with the indicated compounds. Combo, OTX015 combined with GNE-781. Right, bubble plot summarizing the proportion of megadomain overlapping genes downregulated (MD_down) with associated statistical significance of enrichment ($-\log_{10} P$) indicated by the color gradient (red, higher significance; blue, lower). Bubble size is proportional to the fraction (shown in the legend) of megadomain-overlapping genes that are significantly downregulated. OTX, OTX015; NEO, NEO2734; GNE, GNE-781.

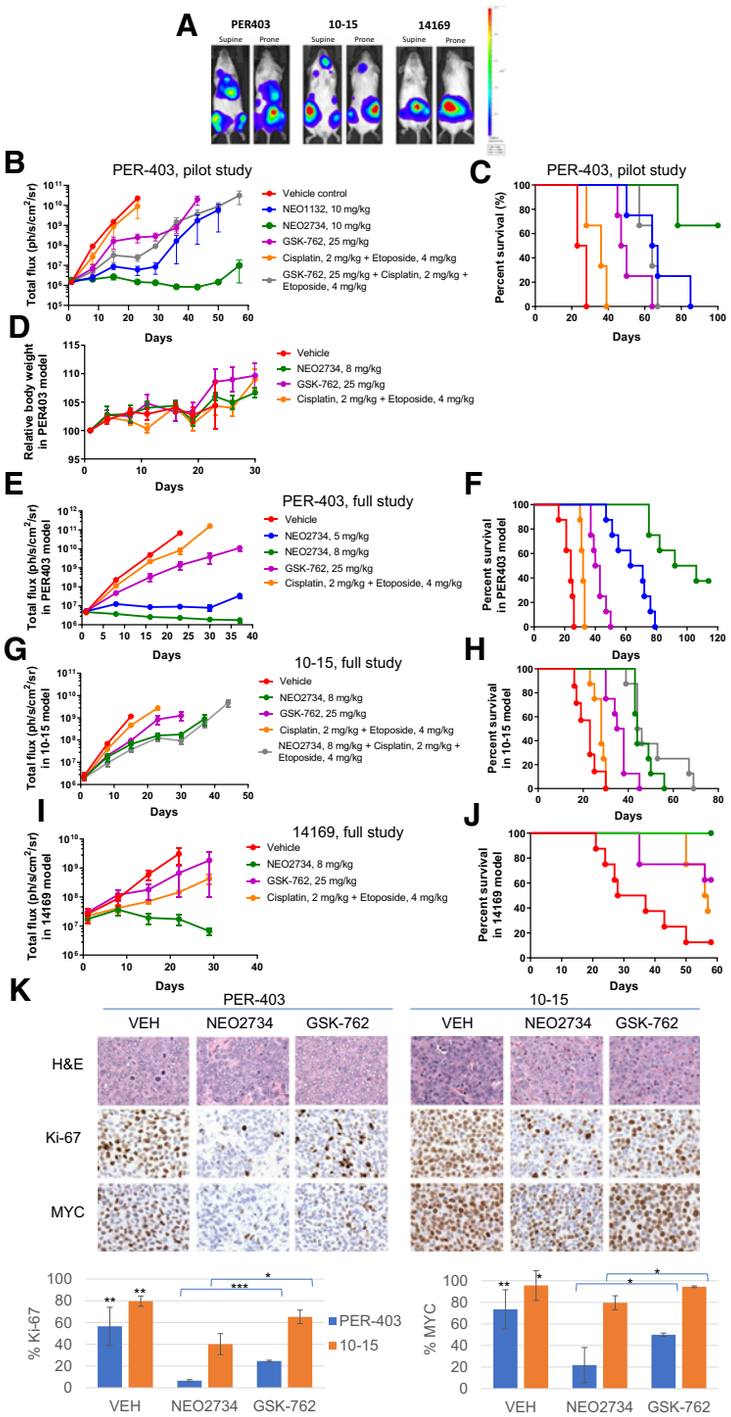

Figure 4.

NEO2734 is superior than lead clinical BET inhibitor or chemotherapy in repressing tumor growth and prolonging survival in preclinical models of NMC. **A,** Representative bioluminescent images (BLI) of the three disseminated xenograft models of NMC used in these preclinical studies. **B,** Tumor growth measured by BLI in the PER-403 model pilot study using $n = 4$ mice per arm. **C,** Kaplan–Meier curve of 103-day survival in the PER-403 pilot study. Start of treatment is day one for all experiments, after measurable tumor is detected in all mice. **D,** Thirty-day relative mouse body weights in the full study using the PER-403 xenograft model depicted for all treatment groups. **E,** Tumor growth in the PER-403 model full study ($n = 8$ mice per arm). **F,** 118-day survival proportions in PER-403 model. **G,** Tumor growth in 10–15 model full study ($n = 8$ mice per arm). **H,** Seventy-day survival in 10–15 model. **I,** Thirty-day growth in the 14169 NMC model, full study ($n = 8$ mice per arm). **J,** Sixty-day survival in the 14169 model. **K,** Top, micrographs of tumor tissue taken from mice 24 hours following the final of three days of daily dosing for the indicated compounds. Shown are H&E and IHC staining using antibodies recognizing the indicated antigens. All photomicrographs were taken at identical magnification (400×) and exposure settings. VEH, vehicle. Bottom, bar graphs of average Ki-67 and MYC percentages across three different mouse samples corresponding with the experiment, top (*, $P < 0.05$; **, $P < 0.01$; ***, $P < 0.0001$). Asterisks above the vehicle (VEH) bars denote comparisons between tissue from vehicle and NEO2734-treated mice.

superior pharmacokinetic (higher target affinity, residence time, bioavailability) properties of NEO2734; or (iii) posttranscriptional effects of NEO2734 that impact BRD4-NUT function. Our demonstration that combining selective BET and p300/CBP bromodomain inhibitors synergistically inhibits growth of NMC cells (**Fig. 1E**), and that NEO2734 induces transcriptional effects of an augmented BET bromodomain inhibition phenotype (**Fig. 3F–H**), supports the concept that cooperative p300/BRD cotargeting confers improved activity. MYC is upregulated by BRD4-NUT, thus the observation that p300/CBP and BET bromodomain inhibitors cooperatively deplete MYC in NMC cells (**Fig. 3G**), and that superior MYC depletion was observed in NEO2734-treated preclinical samples (**Fig. 4K**), again supports the concept of cooperative inhibition of BRD4-NUT.

The second possible characteristic of NEO2734, superior pharmacokinetics, may also explain its greater *in vivo* activity. The higher affinity of NEO2734 for BET bromodomains than i-BET-762 (**Fig. 2B**) might contribute to its superior efficacy *in vivo*, but does not explain its more potent transcriptional effects than OTX015 (**Fig. 3C** and **H**), which has a similar affinity for BRD4 bromodomains (EC_{50} = 10–19 nmol/L; ref. 38). There are other theoretical properties that might confer improved pharmacokinetics of NEO2734, including a higher residence time within BRD4–NUT–p300 complexes, due to its interaction with both BRD4 and p300.

The third potential effect, that of posttranscriptional changes, of NEO2734 that may explain its greater preclinical activity is one of considerable interest because the p300 bromodomain is known to be important in some key protein-protein interactions (20). The p300 bromodomain may be key to its interaction with BRD4-NUT core protein constituents, including BRD4-NUT itself.

In conclusion, we have identified NEO2734 as a highly promising preclinical therapy of NMC to date. Multispecies IND-enabling GLP toxicology studies for NEO2734 have been completed and these data indicate that patients with NMC should be included in initial clinical studies. Better mechanistic understanding of how NEO2734 durably inhibits NMC growth will improve our understanding of BRD4-NUT oncogenic function and lay the groundwork to further improve treatment and understanding of this disease.

Disclosure of Potential Conflicts of Interest

F. Giles is a consultant and has ownership interest (including patents) in Epigene Therapeutics Inc. G.I. Shapiro reports receiving a commercial research grant from Lilly, EMD-Merck Serono, Merck & Co., Sierra Oncology, Pfizer, Array Biopharma, has ownership interest (including patents) in a dosage regimen for sapacitibane and seliciclib (patent), compositions and methods for predicting response and resistance to CDK4/6 inhibition (patent pending), and is a consultant/advisory board member at Lilly, EMD/Merck Serono, Almac, Ipsen, Roche, Angiex, Daiichi Sankyo, Seattle Genetics, Artios, Boehringer Ingelheim, Concarlo, Atrin, Pfizer, Immunomet, Asana, Sierra Oncology, G1 Therapeutics, Bicycle Therapeutics, Fusion Pharmaceuticals, Bayer, Cybrexa Therapeutics, and Astex. P.A. Cole has ownership interest (including patents) in Acylin. C.A. French is a consultant at Boehringer-Ingelheim, Glaxo-Smith-Kline, reports receiving a commercial research grant from Boehringer-Ingelheim and Glaxo-Smith-Kline. No potential conflicts of interest were disclosed by the other authors.

Authors' Contributions

Conception and design: C.D. Morrison-Smith, F. Giles, A. Griffin, B. Brown, P.A. Cole, C.A. French

Development of methodology: C.D. Morrison-Smith, P.C. Gokhale, B.E. Zucconi, C.A. French

Acquisition of data (provided animals, acquired and managed patients, provided facilities, etc.): T.M. Knox, I. Filic, K.M. Soroko, B.K. Eschle, M.K. Wilkens, P.C. Gokhale, B.E. Zucconi, C.A. French

Analysis and interpretation of data (e.g., statistical analysis, biostatistics, computational analysis): C.D. Morrison-Smith, T.M. Knox, I. Filic, K.M. Soroko, M.K. Wilkens, P.C. Gokhale, F. Giles, G.I. Shapiro, P.A. Cole, M.E. Lemieux, C.A. French

Writing, review, and/or revision of the manuscript: C.D. Morrison-Smith, P.C. Gokhale, F. Giles, B. Brown, G.I. Shapiro, P.A. Cole, M.E. Lemieux, C.A. French

Administrative, technical, or material support (i.e., reporting or organizing data, constructing databases): P.C. Gokhale, F. Giles

Study supervision: P.C. Gokhale, P.A. Cole, C.A. French

Acknowledgments

This work was supported by a research grant from the NCI (CA124633, to C.A. French), NIGMS (GM62437, to P.A. Cole; GM124357, to B.E. Zucconi) the Samuel Waxman Cancer Research Foundation (to C.A. French), the St. Baldrick's Foundation (to C.A. French), and the American Cancer Society (to C.D. Morrison-Smith). The authors thank Karen Gascoigne (Genentech Inc.) for sharing GNE-781 with us. We thank Dana-Farber/Harvard Cancer Center in Boston, MA, for the use of the Specialized Histopathology Core, which provided histology and IHC service. Dana-Farber/Harvard Cancer Center is supported, in part, by an NCI Cancer Center Support Grant # NIH 5 P30 CA06516. The authors are grateful to Epigene Therapeutics for providing NEO2734 and NEO1132.

The costs of publication of this article were defrayed in part by the payment of page charges. This article must therefore be hereby marked *advertisement* in accordance with 18 U.S.C. Section 1734 solely to indicate this fact.

Received February 3, 2020; revised March 12, 2020; accepted April 13, 2020; published first May 5, 2020.

References

1. French CA, Kutok JL, Faquin WC, Toretsky JA, Antonescu CR, Griffin CA, et al. Midline carcinoma of children and young adults with nut rearrangement. J Clin Oncol 2004;22:4135–9.
2. French CA, Miyoshi I, Kubonishi I, Grier HE, Perez-Atayde AR, Fletcher JA. Brd4-nut fusion oncogene: A novel mechanism in aggressive carcinoma. Cancer Res 2003;63:304–7.
3. Bauer DE, Mitchell CM, Strait KM, Lathan CS, Stelow EB, Luer SC, et al. Clinicopathologic features and long-term outcomes of nut midline carcinoma. Clin Cancer Res 2012;18:5773–9.
4. Chau NG, Ma C, Danga K, Al-Sayegh H, Sridharan M, Nardi V, et al. An anatomical site and genetic based prognostic model for patients with nut midline carcinoma: analysis of 124 patients. JNCI Cancer Spectr. 2020 Apr; 4(2): pkz094. Published online 2019 Nov 6. doi: 10.1093/jncics/pkz094.
5. Coccia PF. Overview of adolescent and young adult oncology. J Oncol Pract 2019; 15:235–7.
6. French CA. Pathogenesis of nut midline carcinoma. Annu Rev Pathol 2012;7: 247–65.
7. French CA. Nut carcinoma: clinicopathologic features, pathogenesis, and treatment. Pathol Int 2018;68:583–95.
8. Lee JK, Louzada S, An Y, Kim SY, Kim S, Youk J, et al. Complex chromosomal rearrangements by single catastrophic pathogenesis in nut midline carcinoma. Ann Oncol 2017;28:890–7.
9. Grayson AR, Walsh EM, Cameron MJ, Godec J, Ashworth T, Ambrose JM, et al. Myc, a downstream target of brd-nut, is necessary and sufficient for the blockade of differentiation in nut midline carcinoma. Oncogene 2014;33: 1736–42.
10. Alekseyenko AA, Walsh EM, Wang X, Grayson AR, Hsi PT, Kharchenko PV, et al. The oncogenic brd4-nut chromatin regulator drives aberrant transcription within large topological domains. Genes Dev 2015;29:1507–23.
11. Jin Q, Yu LR, Wang L, Zhang Z, Kasper LH, Lee JE, et al. Distinct roles of gcn5/pcaf-mediated h3k9ac and cbp/p300-mediated h3k18/27ac in nuclear receptor transactivation. EMBO J 2011;30:249–62.
12. Reynoird N, Schwartz BE, Delvecchio M, Sadoul K, Meyers D, Mukherjee C, et al. Oncogenesis by sequestration of cbp/p300 in transcriptionally inactive hyperacetylated chromatin domains. EMBO J 2010;29:2943–52.
13. Alekseyenko AA, Walsh EM, Zee BM, Pakozdi T, Hsi P, Lemieux ME, et al. Ectopic protein interactions within brd4 chromatin complexes drive oncogenic megadomain formation in nut midline carcinoma. Proc Natl Acad Sci U S A 2017;114:E4184–92.
14. Stathis A, Zucca E, Bekradda M, Gomez-Roca C, Delord JP, de La Motte Rouge T, et al. Clinical response of carcinomas harboring the brd4-nut oncoprotein to the targeted bromodomain inhibitor otx015/mk-8628. Cancer Discov 2016;6:492–500.
15. Lewin J, Soria JC, Stathis A, Delord JP, Peters S, Awada A, et al. Phase ib trial with birabresib, a small-molecule inhibitor of bromodomain and extraterminal proteins, in patients with selected advanced solid tumors. J Clin Oncol 2018:36;3007–14.
16. Liao S, Maertens O, Cichowski K, Elledge SJ. Genetic modifiers of the BRD4-NUT dependency of NUT midline carcinoma uncovers a synergism between BETis and CDK4/6is. Genes Dev 2018;32:1188–200.
17. Wang R, You J. Mechanistic analysis of the role of bromodomain-containing protein 4 (brd4) in brd4-nut oncoprotein-induced transcriptional activation. J Biol Chem 2015;290:2744–58.

18. Romero FA, Murray J, Lai KW, Tsui V, Albrecht BK, An L, et al. Gne-781, a highly advanced potent and selective bromodomain inhibitor of cyclic adenosine monophosphate response element binding protein, binding protein (cbp). J Med Chem 2017;60:9162–83.
19. Zucconi BE, Makofske JL, Meyers DJ, Hwang Y, Wu M, Kuroda MI, et al. Combination targeting of the bromodomain and acetyltransferase active site of p300/cbp. Biochemistry 2019;58:2133–43.
20. Hou T, Ray S, Lee C, Brasier AR. The STAT3 NH2-terminal domain stabilizes enhanceosome assembly by interacting with the p300 bromodomain. J Biol Chem 2008;283:30725–34.
21. Zucconi BE, Luef B, Xu W, Henry RA, Nodelman IM, Bowman GD, et al. Modulation of p300/CBP acetylation of nucleosomes by bromodomain ligand I-CBP112. Biochemistry 2016;55:3727–34.
22. Toretsky JA, Jenson J, Sun CC, Eskenazi AE, Campbell A, Hunger SP, et al. Translocation (11;15;19): A highly specific chromosome rearrangement associated with poorly differentiated thymic carcinoma in young patients. Am J Clin Oncol 2003;26:300–6.
23. Kees UR, Mulcahy MT, Willoughby ML. Intrathoracic carcinoma in an 11-year-old girl showing a translocation t(15;19). Am J Pediatr Hematol Oncol 1991;13:459–64.
24. Chou TC. Drug combination studies and their synergy quantification using the chou-talalay method. Cancer Res 2010;70:440–6.
25. Yan Y, Ma J, Wang D, Lin D, Pang X, Wang S, et al. The novel bet-cbp/p300 dual inhibitor neo2734 is active in spop mutant and wild-type prostate cancer. EMBO Mol Med 2019;11:e10659.
26. Pourashraf M, Jacquemot G, Claridge S, Bayrakdarian M, Johnstone S, Albert JS, et al., inventors; Neomed Institute, assignee. Substituted benzimidazoles, their preparation and their use as pharmaceuticals. WO/2017/024412. 2017 Feb 16.
27. Jacquemot G, Bayrak-Darian M, Johnstone S, Albert JS, Griffin A, inventors; Neomed Institute, assignee. Aryl-substituted dihydroquinolinones, their preparation and their use as pharmaceuticals. US patent 20180230130. 2018 Aug 16.
28. Piha-Paul SA, Hann CL, French CA, Cousin S, Braña I, Cassier PA, et al. Phase 1 study of molibresib (gsk525762), a bromodomain and extra-terminal domain protein inhibitor, in nut carcinoma and other solid tumors. JNCI Cancer Spectr 2019;4:pkz093.
29. French CA, Ramirez CL, Kolmakova J, Hickman TT, Cameron MJ, Thyne ME, et al. Brd-nut oncoproteins: A family of closely related nuclear proteins that block epithelial differentiation and maintain the growth of carcinoma cells. Oncogene 2008;27:2237–42.
30. French CA, Rahman S, Walsh EM, Kuhnle S, Grayson AR, Lemieux ME, et al. NSD3-NUT fusion oncoprotein in NUT midline carcinoma: Implications for a novel oncogenic mechanism. Cancer Discov 2014;4:928–41.
31. Filippakopoulos P, Qi J, Picaud S, Shen Y, Smith WB, Fedorov O, et al. Selective inhibition of bet bromodomains. Nature 2010;468:1067–73.
32. Jin L, Garcia J, Chan E, de la Cruz C, Segal E, Merchant M, et al. Therapeutic targeting of the cbp/p300 bromodomain blocks the growth of castration-resistant prostate cancer. Cancer Res 2017;77:5564–75.
33. Schwartz BE, Hofer MD, Lemieux ME, Bauer DE, Cameron MJ, West NH, et al. Differentiation of nut midline carcinoma by epigenomic reprogramming. Cancer Res 2011;71:2686–96.
34. Wyce A, Degenhardt Y, Bai Y, Le B, Korenchuk S, Crouthame MC, et al. Inhibition of bet bromodomain proteins as a therapeutic approach in prostate cancer. Oncotarget 2013;4:2419–29.
35. Ito K, Hanamura T, Murayama K, Okada T, Watanabe T, Harada M, et al. Multimodality therapeutic outcomes in anaplastic thyroid carcinoma: Improved survival in subgroups of patients with localized primary tumors. Head Neck 2012;34:230–7.
36. Stevens TM, Morlote D, Xiu J, Swensen J, Brandwein-Weber M, Miettinen MM, et al. Nutm1-rearranged neoplasia: A multi-institution experience yields novel fusion partners and expands the histologic spectrum. Mod Pathol 2019;32:764–73.
37. Beesley AH, Stirnweiss A, Ferrari E, Endersby R, Howlett M, Failes TW, et al. Comparative drug screening in nut midline carcinoma. Br J Cancer 2014;110:1189–98.
38. Noel JK, Iwata K, Ooike S, Sugahara K, Nakamura H, Daibata M. Development of the bet bromodomain inhibitor otx015 [abstract]. In: Proceedings of the AACR-NCI-EORTC International Conference: Molecular Targets and Cancer Therapeutics; 2013 Oct 19–23; Boston, MA. Philadelphia (PA): AACR; 2013. Abstract nr C244.